

# Ethylene Carbonate Free Sulfone-Based Electrolyte for Enabling Superior Performance of High Ni-containing Li-Transition Metal Oxide Cathodes at High Voltage and High Temperature

Arpita Das<sup>+</sup><sup>[a]</sup> Mohammed Riyaz<sup>+</sup><sup>[a]</sup> Sushobhan Kobi,<sup>[a]</sup> Dipannita Saha,<sup>[a]</sup> and Amartya Mukhopadhyay\*<sup>[a]</sup>

The present study introduces an ethylene carbonate (EC) free electrolyte, composed of 1 M LiPF<sub>6</sub> in ethyl methyl sulfone (EMS) and dimethyl carbonate (DMC) (3:7 by volume), for Li-ion batteries, which is better suited for usage with higher upper cut-off potentials, with high Ni-containing 'layered' Li-transition metal oxide cathodes (like Li-NMC811), and at elevated temperature. The as-designed and developed sulfone-based electrolyte exhibits superior anodic stability and lower electrolyte resistance, while suppressing the decomposition of LiPF<sub>6</sub> and facilitating the formation of a S-containing, more passivating, thinner and uniform CEI layer on Li-NMC811, despite the usage

of a high upper cut-off potential of 4.5 V (vs. Li/Li<sup>+</sup>). Compared with conventional EC-based electrolyte, the sulfone-based electrolyte results in notably suppressed rise in impedance and improved cyclic-stability, with capacity retentions of ~87% (vs. ~78% for EC-based electrolyte) after 50 cycles @ C/10 at room temperature (going up to 4.5 V). Even at 45 °C, the sulfone-based electrolyte results in significantly higher initial Coulombic efficiency (*viz.*, >80% vs. ~40%), higher reversible capacity (~230 mAh/g vs. ~178 mAh/g) and superior cyclic stability (~74% vs. ~46% retention after 50 cycles @ C/10); thus, revealing its superiority for usage at elevated temperature.

## Introduction

Lithium-ion batteries (LIBs) have garnered widespread attention due to their applicability in diverse fields, ranging from consumer electronic devices to renewable energy storage solutions to electric vehicles. The evolution of high nickel-containing 'layered' Li-transition metal (T<sub>M</sub>) oxide based cathodes (such as, LiNi<sub>(1-x-y)</sub>Mn<sub>x</sub>Co<sub>y</sub>O<sub>2</sub> or Li-NMC; with Ni $\geq$ 0.8) and the requirement of stable high-voltage electrochemical cycling are closely linked with the pursuits for higher energy density and lower cost (due to minimization/removal of Co-content), as is needed for the next-generation LIBs.<sup>[1]</sup> The energy density is proportional to the specific capacity and cell voltage; which renders the capability of stable operation at high cell voltages an important requirement towards enhancing energy density. At present, the operation voltage of a cell is primarily limited by the electrochemical stability window of the electrolyte, which plays a dominant role towards achievable energy density, electrochemical performance and safety aspects, especially for the high Ni-containing Li-T<sub>M</sub>-oxides.<sup>[1,2]</sup> The electrolyte also influences the operation at higher temperatures (*i.e.*, beyond ambient temperature of ~24–25 °C), which is very

important for usage in tropical/sub-tropical climates. At present, the commercially used liquid electrolyte contains LiPF<sub>6</sub> salt dissolved in two (or more) types of aliphatic carbonate solvents; *viz.*, cyclic carbonates such as ethylene carbonate (EC), which have a high dielectric constant and ensure salt dissociation, and linear carbonates such as dimethyl carbonate (DMC), diethyl carbonate (DEC), and ethyl methyl carbonate (EMC), which have low viscosities and, thus, help achieve an appropriate ionic conductivity.<sup>[3,4]</sup> Among these, EC, which has a high dielectric constant, low volatility, and excellent thermal stability, is a solvent commonly used in LIBs having cathode based on high Ni-containing 'layered' Li-T<sub>M</sub>-oxides, such as Li-NMC811 (*i.e.*, LiNi<sub>0.8</sub>Mn<sub>0.1</sub>Co<sub>0.1</sub>O<sub>2</sub>).

In such high Ni-containing cathodes nickel is present primarily in the +3 oxidation state, which goes to +4 state during charging (or electrochemical Li-removal). The low thermal tolerance of Ni<sup>+4</sup> in the charged state, especially when in contact with the highly reductive EC, causes instability and serious safety hazards. As per one of the schools of thought, EC is oxidized at the surface of the charged cathode by dehydrogenation to yield H<sup>+</sup> and e<sup>-</sup>. This H<sup>+</sup> can take-up lattice oxygen, resulting in an increase in impedance, and react with electrolyte salts to form products that accelerate T<sub>M</sub>-dissolution.<sup>[5,6]</sup> Furthermore, at such high voltages (*i.e.*, >4.2 V vs. Li/Li<sup>+</sup>), deleterious/irreversible surface structural changes of such cathode materials also take place as a result of parasitic reactions between the delithiated cathodes and electrolytes; which, in turn, increases cathode impedance and eventually degrades the cell's electrochemical performance during charge/discharge cycles. At such high voltages, the oxidizable electrolytes easily seize oxygen from the delithiated cathode, accelerating surface reconstruc-

[a] A. Das,<sup>+</sup> M. Riyaz,<sup>+</sup> Dr. S. Kobi, D. Saha, Prof. A. Mukhopadhyay  
Advanced Batteries and Ceramics Laboratory  
Department of Metallurgical Engineering and Materials Science  
Indian Institute of Technology Bombay  
Mumbai 400076, India  
E-mail: amartya\_mukhopadhyay@iitb.ac.in

<sup>†</sup> Equal contributions.

 Supporting information for this article is available on the WWW under  
<https://doi.org/10.1002/batt.202400608>

tion and side reactions. Accordingly, developing EC-free high-voltage electrolytes that can suppress the electrolyte oxidation, block parasitic reactions, suppress cathode surface reconstruction and  $T_m$ -dissolution is the most practical/effective way forward towards further improving the energy density of the Li-ion cells, without compromising on the electrochemical performance and safety aspects. However, developing/selecting an electrolyte with high anodic stability, broad electrochemical window, low viscosity and suitable ionic conductivity, despite being very important, is still a challenge for rendering the successful usage of high Ni-containing  $\text{Li}-\text{T}_m\text{-oxide}$  based cathodes and accessing high cell voltages.

In this regard, a sulfone-based high-voltage stable liquid electrolyte has been designed and developed here. The sulfonyl group in the sulfone-based electrolyte has a stronger electron drawing tendency, which lowers the energy level of the Highest Occupied Molecular Orbital (HOMO) of the electrolyte, resulting in higher oxidation stability, high dielectric permittivity, elevated anodic stability and low flammability<sup>[7–11]</sup> (see Table S1 in Supplementary Information file, SI, for the relevant physical properties of various organic solvents that are commonly used as LiB electrolytes). As will be presented in this communication, the newly-developed sulfone-based electrolyte bestows superior cathode electrolyte interface (CEI) characteristics, lower impedance and, thus, superior cyclic stability to  $\text{Li}-\text{NMC811}$  cathode during high voltage cycling, as well as facilitates stable high temperature cell operation.

## Experimental Section

The EC free, sulfone-containing electrolyte was prepared by dissolving  $\text{LiPF}_6$  as the Li salt in EMS:DMC solvent (in 1:1, 3:7 and 1:9 by volume). 0.7595 g of  $\text{LiPF}_6$  salt was dissolved in 5 mL of solvent with EMS:DMC (with varying volumetric ratio of 1:1, 3:7 and 1:9) to obtain 1 M  $\text{LiPF}_6$  in the electrolytes. This solution was stirred using a magnetic stirrer for 12 h to obtain uniform dissolution of the electrolyte components. The electrolyte salt  $\text{LiPF}_6$  ( $\geq 99.99\%$ ), and the solvent DMC ( $\geq 9.9\%$ ) were sourced from Sigma Aldrich and solvent EMS ( $> 98\%$ ) from Tokyo Chemical Industry. The electrolyte solutions were prepared inside an Ar-filled glove-box (MBraun Unilab Pro), having  $\text{H}_2\text{O}$  and  $\text{O}_2$  levels below 0.1 ppm.

X-ray photoelectron spectroscopy (XPS, AXIS Supra) with an Al  $\text{K}\alpha$  radiation (1486.6 eV) excitation source was employed to examine the surface chemistry of the electrodes before and after cycling. Features of the CEI after 1 cycle was looked into using high-resolution transmission electron microscopy (HRTEM), Thermo Scientific, Themis 300 G. The surface feature of the electrodes before and after cycling were observed using FEG-SEM (JEOL-JSM 7600F). Powder X-Ray diffraction (XRD) measurements of the electrodes before and after cycling were carried out using PANalytical X'Pert X-ray diffractometer, using Cu  $\text{K}\alpha$  radiation, at scan rate of 1 °/min.

The working electrodes for the Li 'half' cells were prepared by mixing commercial  $\text{Li}-\text{NMC811}$  (MTI Corporation) as the active material with carbon black (Super P; as conducting additive; from Alfa Aesar) and PVDF binder (Sigma Aldrich) in NMP (Sigma Aldrich) as the solvent in a mass ratio of 8:1:1. The slurries were tape casted onto a carbon-coated aluminum foil (Batsol), followed by drying in a vacuum oven at 90 °C for 12 h to remove the solvent.

The dried foil was then calendered at 50 °C. The mass of the active electrode material was  $\sim 3 \text{ mg/cm}^2$ . Standard CR2032 coin cells were assembled in the Ar-filled glove box (having  $\text{H}_2\text{O}$  and  $\text{O}_2$  levels  $< 0.1 \text{ ppm}$ ) with the as-prepared working electrode, metallic Li as the counter-cum-reference electrode, Whatman glass fiber filter (GF/D) as separator and 1 M  $\text{LiPF}_6$  in EMS:DMC (in the various ratios by volume) as the electrolyte. Similar cells were also assembled with commercial grade 1 M  $\text{LiPF}_6$  in EC:DEC:DMC (1:1:1 by volume) as the electrolyte for control experiments.

Anodic stability studies were conducted using a potentiostat/galvanostat (Biologic; BCS 810) within the potential window of 2.5–5.5 V (versus  $\text{Li}/\text{Li}^+$ ) with Al as the working electrode and Li metal as the counter-cum-reference electrode. Electrochemical Impedance Spectroscopy (EIS) was carried out using the same potentiostat/galvanostat in the frequency range of 1 Hz–10 kHz with symmetric cell having stainless steel spacer on both the sides. Galvanostatic cycling runs were performed using NEWARE battery tester at a current density equivalent to C/10 (C-rate estimated considering theoretical cathode capacity as 200 mAh g<sup>-1</sup>) within a cell voltage window of 2.5–4.5 V with the as-prepared working electrode, metallic Li as the counter-cum-reference electrode.

## Results and Discussion

The newly designed EC-free sulfone-based electrolyte in here consists of 1 M  $\text{LiPF}_6$  salt dissolved in a solvent with a high dielectric constant, viz., ethyl methyl sulfone (EMS), and a diluent, viz., dimethyl carbonate (DMC), in the ratios of 1:1, 3:7, and 1:9. The anodic stability of these electrolytes, which strongly depends on the nature of the solvent and salts, was determined via linear sweep voltammetry (LSV) from 2.5 to 5.5 V vs.  $\text{Li}/\text{Li}^+$  at a potential scan rate of 0.05 mV/s in a Li//electrolyte//Al cell configuration (see Figure 1a). Among the as-tested EMS-containing electrolytes, the anodic stability window is seen to increase with EMS-content, followed by decrease. The EMS:DMC 3:7 based electrolyte exhibits current onset potential beyond 4.6 V and a significantly suppressed oxidative current (see Figure 1b), with the EMS:DMC 1:1 and 1:9 based compositions exhibiting onset potentials of 4.2 and 4.38 V, respectively, under the same conditions. In this regard, the 1 M  $\text{LiPF}_6$  in sulfone-based EMS:DMC 3:7 electrolyte is taken as an optimized composition. The conductivities of the sulfone-based electrolytes were measured via electrochemical impedance spectroscopy (EIS) in the frequency range of 1 Hz to 10 kHz, with the Nyquist plots shown in Figure 1c. The electrolyte bulk resistance initially decreases with increasing EMS content owing to the higher dielectric constant facilitating better ion solvation and higher salt dissociation. Again, the lowest electrolyte resistance has been observed for EMS:DMC 3:7, which is  $\sim 3.6 \Omega$  (see Figure 1d), and which is also lower than that of a more usual/standard EC-containing electrolyte, viz., 1 M  $\text{LiPF}_6$  in EC:DEC:DMC 1:1:1, which has been found to possess a resistance of  $\sim 7.4 \Omega$  under the same conditions. With further increase in the EMS content, the electrolyte resistance increases due to increased viscosity, indicating that EMS:DMC 3:7 is, again, the optimal solvent composition.

Figures 2a and d compare the EIS spectra obtained with the EC-free sulfone-based EMS:DMC 3:7 and the more usual/

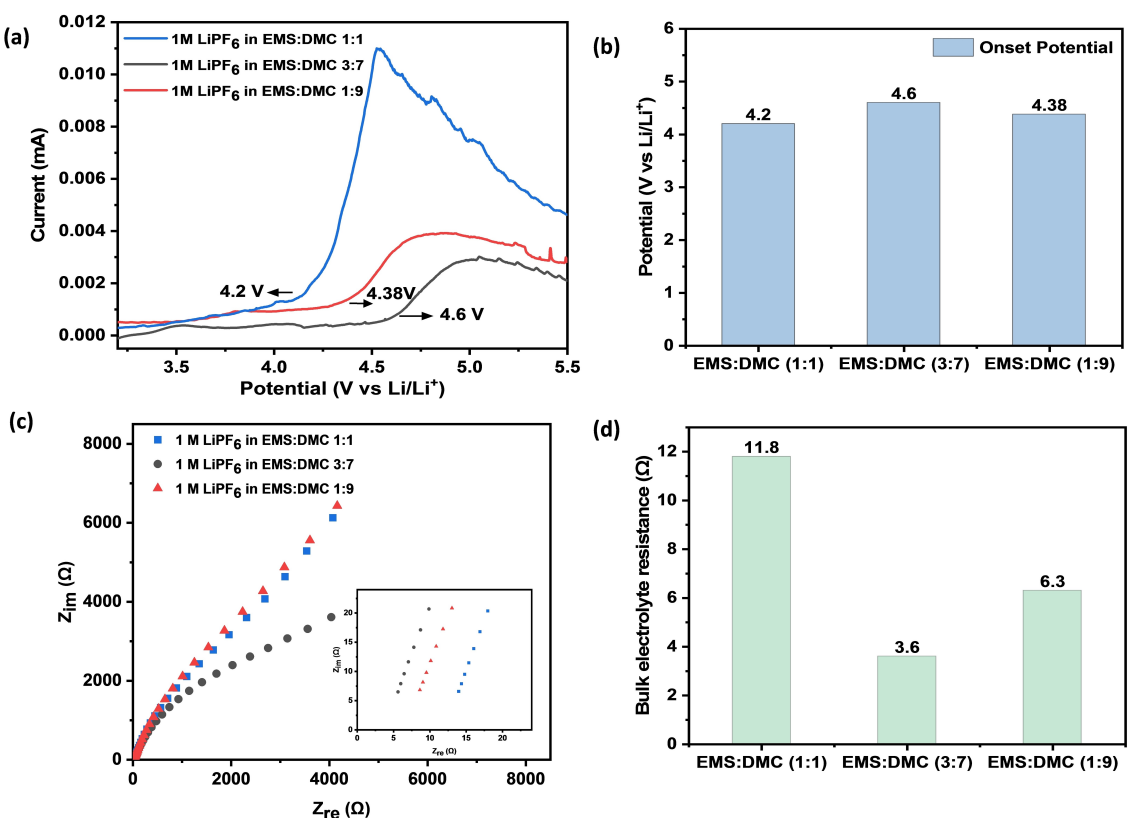


**Figure 1.** (a) Anodic stability and (b) onset of oxidative current of the as-designed sulfone-based electrolytes (*i.e.*, 1 M LiPF<sub>6</sub> in EMS:DMC *xy*), as tested via linear sweep voltammetry (@ 0.05 mV/s) with Al as the working electrode and Li metal as the counter-cum-reference electrode, (c) Nyquist (EIS) plot and (d) Comparison of bulk electrolyte resistances of the sulfone-based electrolytes.

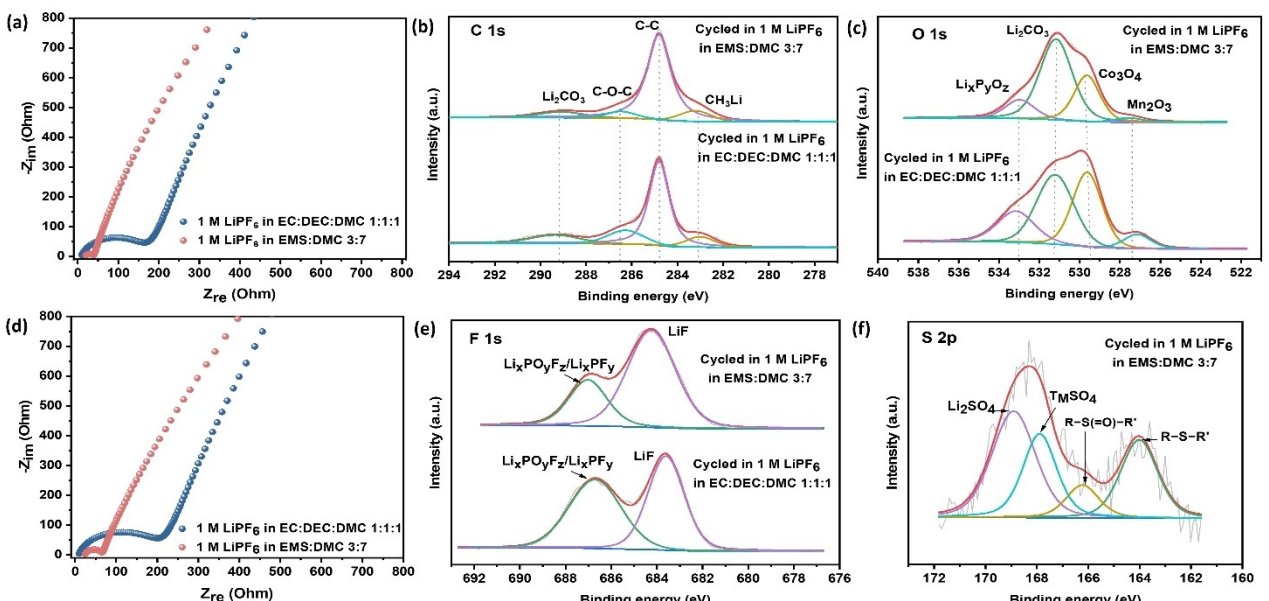


**Figure 2.** Nyquist (EIS) plots for Li/Li–NMC811 cells cycled with the standard EC-based EC:DEC:DMC 1:1:1 and the newly-developed sulfone-based EMS:DMC 3:7 electrolytes after (a) 1 cycle @ C/10 and (d) 2 cycles @ C/10. XPS spectra for (b) C 1s, (c) O 1s, (e) F 1s, (f) S 2p from the CEIs formed on the Li–NMC811 electrodes when cycled with EC:DEC:DMC 1:1:1 and sulfone-based EMS:DMC 3:7 electrolytes for 50 cycles @ C/10.

standard EC:DEC:DMC 1:1:1 electrolytes (both having 1 M LiPF<sub>6</sub>) after 1 and 2 galvanostatic cycles @ C/10 in a Li–NMC811 ‘half’ cell configuration. The Nyquist plots present

depressed semicircles in the high-frequency region, corresponding to interfacial impedance, including the surface film resistance and charge transfer resistance, and a sloped line in the

low-frequency region, representing the Warburg impedance.<sup>[10]</sup> The corresponding EIS data were fitted with the equivalent circuit model, as in Figure S1. After the 1<sup>st</sup>, as well as the 2<sup>nd</sup>, cycle, the cell containing the new sulfone-based electrolyte exhibited lower interfacial impedance (*viz.*, by factors of ~0.13 and ~0.24 post cycle 1 and 2, respectively), as compared to those with the standard EC:DEC:DMC-based electrolyte, hinting at the formation of a more stable cathode electrolyte interface (CEI) layer on the Li–NMC811 electrode surface, as well as suppressed damage of the structure at the surface of the cathode material.

To gain more information about the interfacial films or CEI, Figures 2b–f compare the XPS spectra obtained with the Li–NMC811 electrodes cycled with the newly developed sulfone-based EMS:DMC 3:7 and the standard EC:DEC:DMC-based electrolytes. The C 1s spectra (Figure 2b) shows peaks at ~284.8, ~286.3 ± 0.1, ~283 ± 0.2, and ~289.2 eV, which are assigned to C–C (from SP), C–O–C, CH<sub>3</sub>Li (from electrolyte decomposition products),<sup>[12–14]</sup> and Li<sub>2</sub>CO<sub>3</sub> (from electrolyte decomposition products),<sup>[14,15]</sup> respectively. Compared with the ones obtained after cycling with the standard electrolyte, the peaks representing CH<sub>3</sub>Li and Li<sub>2</sub>CO<sub>3</sub> are considerably suppressed in the spectra obtained upon cycling with the new sulfone-based electrolyte, confirming the suppression of decomposition of carbonate-based solvents in the case of the later. Again, in the O 1s spectra (Figure 2c), stronger signals at ~533 ± 0.3, ~531, ~529.6 and ~527 ± 0.5 eV (which correspond to Li<sub>x</sub>P<sub>y</sub>O<sub>z</sub>, Li<sub>2</sub>CO<sub>3</sub>, Co<sub>3</sub>O<sub>4</sub> and Mn<sub>2</sub>O<sub>3</sub>, respectively)<sup>[14,16,17]</sup> have been obtained when cycled with the standard electrolyte than with the sulfone-based counterpart. As for the F 1s spectra, Figure 2e shows two peaks centered at ~684 and ~687 eV, belonging to LiF and Li<sub>x</sub>PO<sub>y</sub>F<sub>z</sub>/Li<sub>x</sub>PF<sub>y</sub>, respectively.<sup>[18]</sup> The intensities of the peaks upon cycling with the sulfone-based electrolyte are significantly lower than with the standard electrolyte, indicating that the decomposition of LiPF<sub>6</sub> was effectively suppressed with the addition of ethyl methyl sulfone. In the S 2p spectra (Figure 2f), as obtained upon cycling with the sulfone-based electrolyte, the peaks centered at ~164, ~166, ~167.7 and ~169 eV belong to alkyl sulfide species (R–S–R'),<sup>[17]</sup> sulfoxides (R–S(=O)–R'),<sup>[19]</sup> T<sub>M</sub>SO<sub>4</sub><sup>[20]</sup> and Li<sub>2</sub>SO<sub>4</sub>,<sup>[17,21]</sup> respectively. It has been reported that S-based compounds, such as, alkyl sulfide species, Li<sub>2</sub>SO<sub>4</sub>, possess excellent passivating properties and also can improve the ionic conductivity of the interfacial films.<sup>[21,22]</sup>

To obtain more direct visualization of the CEI layers, high resolution TEM imaging was done with the cathode-active particles after 1 full cycle @ C/10 in Li ‘half’ cells with the two electrolyte types; see Figure 3. The CEI layer in the case of the EC-based electrolyte (EC:DEC:DMC 1:1:1) was found to be non-uniform even just after one cycle, with the thickness ranging from ~8 to ~56 nm. By contrast, the CEI layer formed upon usage of the sulfone-based EMS:DMC 3:7 electrolyte was found to much more uniform and thinner, with the thickness lying between ~3–6 nm. Nevertheless, the CEI layer thicknesses/uniformity has been found to depend on the EMS content in the new electrolytes, with the thickness being ~4–48 nm and ~8–20 nm for EMS:DMC 1:9 and 1:1, respectively, after 1 full

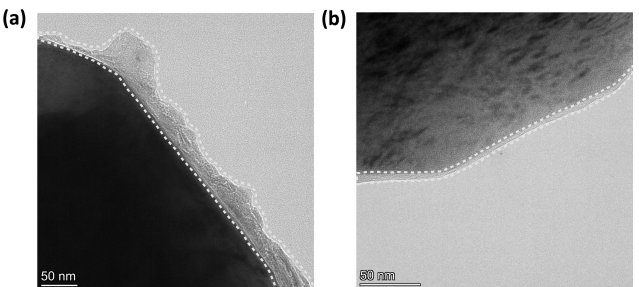


**Figure 3.** HRTEM images of Li–NMC811 electrode-active particles after being subjected to 1 full charge/discharge cycle in Li ‘half’ cells at room temperature, with 1 M LiPF<sub>6</sub> in (a) EC:DEC:DMC (1:1:1) and (b) sulfone-based EMS:DMC (3:7) electrolytes.

charge/discharge cycle (see Figure S2 in SI). Hence, even for this aspect, the 1 M LiPF<sub>6</sub> in EMS:DMC 3:7 electrolyte has been found to be optimal towards facilitating the formation of a thinner and more uniform CEI among all the studied EMS:DMC ratios; thus, leading to the best improved electrochemical performances. Overall, the XPS results, in combination with the EIS and HRTEM results, indicate the formation of a relatively thinner, more uniform and expectedly more conducting CEI on Li–NMC811 cathode when cycled in the newly-developed sulfone-based electrolyte (1 M LiPF<sub>6</sub> in EMS:DMC 3:7); thus, potentially improving the electrochemical performance.

The initial electrochemical performance of the Li–NMC811 cathode in the sulfone-based electrolyte varies slightly with the EMS:DMC ratios, exhibiting initial discharge capacities of ~212 mAh/g, ~210 mAh/g and ~208 mAh/g for EMS:DMC 1:1, 3:7, and 1:9, respectively, with corresponding first cycle Coulombic efficiencies (CE) being ~89%, ~91%, and ~85% (see Figure S3 in SI). These results suggest that the 1 M LiPF<sub>6</sub> EMS:DMC 3:7 facilitates an optimal balance between improved initial discharge capacity and CE, the latter being also important for cyclic stability. Figure 4a presents the electrochemical performance of Li–NMC811 cathode when tested with the newly designed EC-free sulfone-based EMS:DMC 3:7 and standard/usual EC-based EC:DEC:DMC 1:1:1 electrolytes (both having 1 M LiPF<sub>6</sub> as the salt; and no additive) @ C/10 within 2.5–4.5 V (vs. Li/Li<sup>+</sup>) at room temperature (RT) (with the potential profiles in Figures S4a, b in SI). Here, from a practical perspective, the significant result is that, under similar conditions, the capacity retentions obtained after 50 galvanostatic cycles @ C/10 is higher (*viz.*, ~87%) in the case of the new sulfone-based electrolyte, as compared to with the standard electrolyte (*viz.*, ~78%). This immediately indicates that the newly developed EMS:DMC 3:7 based electrolyte bestows enhanced stability towards the electrochemical cycling of high Ni-containing Li–TM-oxide cathode at RT, even upon using a high upper cut-off potential of 4.5 V vs. Li/Li<sup>+</sup>. Even at a higher current density corresponding to 1 C, the Li–NMC811 cathode exhibited a 1<sup>st</sup> cycle reversible/discharge capacity of ~194 mAh/g and cyclic stability pertaining to ~81% capacity retention after 50 cycles at RT with the sulfone-based electrolyte (see Figure S5 in SI).

The effect of the two electrolytes were also compared at an elevated temperature of 45 °C (see Figure 4b and Figures S6a, b

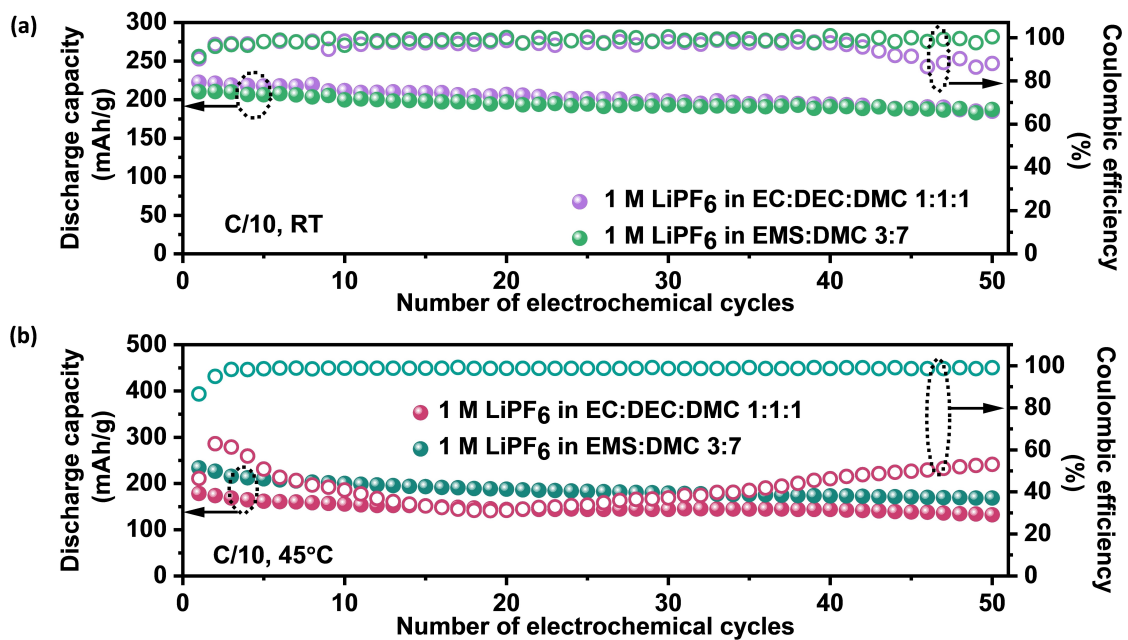


**Figure 4.** (a) Cyclic stability, *i.e.*, reversible Li-storage capacity vs. cycle number (including coulombic efficiency), as obtained upon galvanostatic cycling of Li//Li-NMC811 cells @ C/10 for 50 cycles with EC:DEC:DMC 1:1:1 and sulfone-based EMS:DMC 3:7 based electrolytes at (a) room temperature (RT) and (b) 45 °C.

in SI). Again, the cells containing the sulfone-based electrolyte exhibited a higher initial discharge capacity, as well as capacity retention, of ~230 mAh/g and ~74%, respectively, when compared with just ~178 mAh/g and ~46%, respectively, in the case of the standard EC:DEC:DMC-based electrolyte. Furthermore, upon usage of the standard electrolyte very low initial CE (of ~40%) and discharge capacity were obtained, along with fluctuations and concomitant poor CE right from the very beginning and all along (with CE even reaching ~20% in the intermediate cycles) at this higher temperature (see Figure 4b and Figure S6a in SI). By contrast, in the presence of EMS:DMC 3:7, stable-cum-smooth potential profiles, capacity and CE were obtained, with CE reaching ~100% in 3 cycles and remaining stable thereafter, similar to at RT. This proves that, while exacerbated deleterious interfacial reactions take place at elevated temperature upon usage of the usual EC:DEC:DMC 1:1:1 solvent, leading to immense instability, EMS:DMC 3:7 offers stability and addresses the above problems in significant terms. Hence, the newly developed EC-free sulfone-based

electrolyte is suitable for usage with high Ni-containing Li-T<sub>M</sub>-oxide cathodes even at elevated temperatures, unlike the more usual EC-containing carbonate-based electrolytes.

The electrode surfaces post 50 galvanostatic cycles at RT were checked using SEM (see Figure 5), which indicate that the one cycled using the standard EC:DEC:DMC-based electrolyte suffered from significant damages in the forms of cracks, but not the one cycled using the EMS:DMC-based electrolyte; *viz.*, no notable crack/damage for the later after 50 cycles under the same conditions. Similar observations were made also after 50 cycles at 45 °C (see Figure S7 in ESI). These indicate that the newly developed EC-free sulfone-containing electrolyte suppresses the loss in integrity of the active material and/or cathode electrolyte interface (CEI) film in significant terms despite usage of a high upper cut-off potential of 4.5 V vs. Li/Li<sup>+</sup>, both at room temperature and elevated temperature. Of course, this is in sync with the superior cyclic stability of bestowed by the new electrolyte.

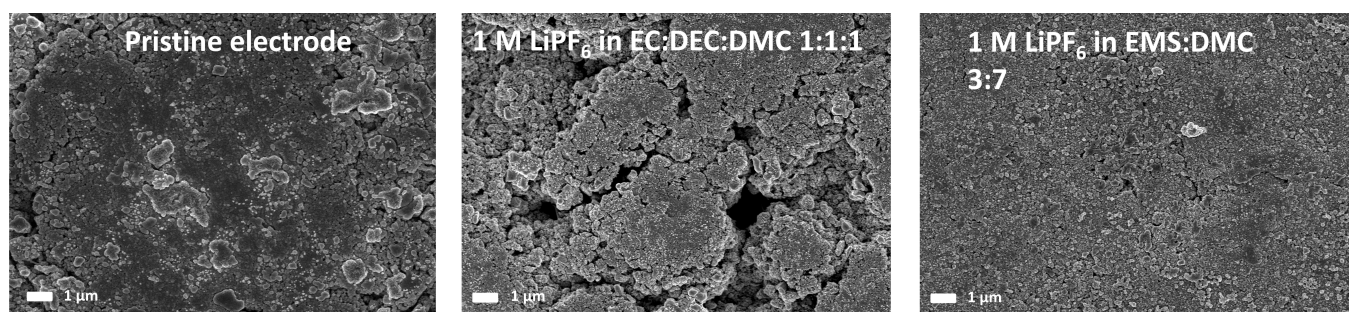


**Figure 5.** SEM images of pristine Li-NMC811 electrode and Li-NMC811 electrodes post 50 cycles @ C/10 at RT in Li//Li-NMC811 ‘half’ cells having the EC:DEC:DMC 1:1:1 and EMS:DMC 3:7 based electrolytes.

Furthermore, XRD of the 50 times cycled Li–NMC811 electrode with standard EC:DEC:DMC-based electrolyte indicates reduction of the I(003)/I(104) peak intensity ratio to ~1 (from the initial ~1.3) due to cation-mixing and possible formation of spinel/rocksalt structure during Li-extraction going up to 4.5 V (not unexpected). Here, it is important to note that such structural damage gets relatively suppressed upon usage of the new EMS:DMC-based electrolyte, as inferred from the slightly higher I(003)/I(104) peak intensity ratio of ~1.1, along with more distinct splitting of (006) and (012) peaks, of the 50 times cycled Li–NMC811 electrode under the same conditions (as in Figure S8 in SI). This indicates that the newly-developed EMS:DMC 3:7 based electrolyte helps better in preserving the structure at the cathode particle surface even upon deep delithiation, possibly due the formation of a more suitable/stable S-containing CEI (as per the XPS and HRTEM results); which also contributes towards the superior cyclic stability obtained with this electrolyte.

## Conclusions

The present work reports the development of a high-voltage stable EC-free electrolyte, which is composed of 1 M LiPF<sub>6</sub> in ethyl methyl sulfone (EMS) and dimethyl carbonate (DMC) (3:7, by volume), as a superior alternative to the more standard EC-based electrolytes. The higher oxidative stability of sulfone bestows this electrolyte with a wider electrochemical stability window, rendering it better suited for usage with higher upper cut-off cell voltages (as are needed for enhancing energy density of Li-ion cells), with the higher dielectric constant of sulfone resulting in lower electrolyte resistance for the optimized EMS:DMC 3:7 solvent. Li//Li–NMC811 ‘half’ cells containing this newly-developed electrolyte exhibit lower impedance (by a factor of ~4) and superior cyclic stability during high voltage cycling with 4.5 V as the upper cut-off potential (*viz.*, 87% vs. 78% capacity retention after 50 cycles @ C/10 at room temperature) when compared with the usage of a more standard/usual EC:DEC:DMC 1:1:1 based electrolyte. Even at 1 C, a discharge capacity of ~194 mAh/g and cyclic stability pertaining to ~81% capacity retention after 50 cycles at RT could be obtained with the sulfone-based electrolyte. XPS reveals suppressed decomposition of LiPF<sub>6</sub> and the formation of a more passivating S-containing CEI layer upon cycling with the EMS:DMC-based electrolyte, with HRTEM revealing the formation of a thinner and more uniform CEI layer. This, along with better preservation of the surface structure of the high Ni-containing Li–NMC811 cathode-active particle (in terms of lesser cation-mixing), facilitates the superior cyclic stability upon usage of this newly-developed electrolyte. Even at higher temperature, *i.e.*, at 45 °C, the 1 M LiPF<sub>6</sub> in EMS:DMC 3:7 electrolyte facilitates significantly higher initial Coulombic efficiency (*viz.*, >80% vs. ~40%), higher reversible capacity (~230 mAh/g vs. ~178 mAh/g) and superior cyclic stability (~74% vs. 46% retention after 50 cycles @ C/10) of Li–NMC811 electrode, when compared with the usage of 1 M LiPF<sub>6</sub> in EC:DEC:DMC 1:1:1 electrolyte; which (*i.e.*, the latter), rather led to

excessive fluctuations in the potential profiles and CE in almost all cycles due to exacerbated surface reactions at the elevated temperature. Hence, the newly designed and developed 1 M LiPF<sub>6</sub> in EMS:DMC 3:7 electrolyte is not only better suited than the usual EC-containing carbonate-based electrolytes for usage with the high Ni-containing ‘layered’ Li–T<sub>M</sub>-oxide cathode materials up to high upper cut-off potentials (in the pursuit for higher energy density), but also for usage at elevated temperatures (at least up to 45 °C), which better suits the tropical/sub-tropical regions.

## Acknowledgements

AM acknowledges CoE-OGE, IIT Bombay, for financial support; and SAIF, and ICCF (IIT Bombay) for enabling the usage of some of the experimental/analytical facilities.

## Conflict of Interests

The authors declare no conflict of interest.

## Data Availability Statement

The data that support the findings of this study are available from the corresponding author upon reasonable request.

**Keywords:** EC-free electrolyte • Li–NMC811 • sulfone-based electrolyte • high voltage • LIBs

- [1] Z. Guo, Z. Cui, R. Sim, A. Manthiram, *Small* **2023**, *19*, 2305055.
- [2] M. Yi, L. Su, A. Manthiram, *J. Mater. Chem. A* **2023**, *11*, 11889–11902.
- [3] W. Li, E. M. Erickso, A. Manthiram, *Nat. Energy* **2020**, *5*, 26–34.
- [4] J. Kalhoff, G. G. Eshetu, D. Bresser, S. Passerini, *ChemSusChem* **2015**, *8*, 2154–2175.
- [5] J. Jiang, J. R. Dahn, *Electrochim. Acta* **2004**, *49*, 4599.
- [6] Y. Zhang, Y. Katayama, R. Tatara, L. Giordano, Y. Yu, D. Fragedakis, J. G. Sun, F. Maglia, R. Jung, M. Z. Bazant, Y. Shao-Horn, *Energy Environ. Sci.* **2020**, *13*, 183–199.
- [7] A. T. S. Freiberg, M. K. Roos, J. Wandt, R. de Vivie-Riedle, H. A. Gasteiger, *J. Phys. Chem. A* **2018**, *122*, 8828–8839.
- [8] K. Xu, C. A. Angell, *J. Electrochem. Soc.* **2002**, *149*, A920–A926.
- [9] X. G. Sun, C. A. Angell, *Electrochim. Commun.* **2005**, *7*, 261–266.
- [10] X. Fan, C. Wang, *Chem. Soc. Rev.* **2021**, *50*, 10486–10566.
- [11] S. S. Zhang, *J. Energy Chem.* **2020**, *41*, 135–141.
- [12] T. Li, J. Zou, Y. Xiao, Y. Li, W. Wang, T. Zhang, *J. Alloys Compd.* **2024**, *999*, 175060.
- [13] R. Dedryvère, H. Martinez, S. Leroy, D. Lemordant, F. Bonhomme, P. Biensan, D. Gonbeau, *J. Power Sources* **2007**, *174*, 462–468.
- [14] F. Wu, G. T. Kim, T. Diemant, M. Kuenzel, A. R. Schür, X. Gao, S. Passerini, *Adv. Energy Mater.* **2020**, *10*, 2001830.
- [15] W. Zhao, J. Zheng, L. Zou, H. Jia, B. Liu, H. Wang, J. G. Zhang, *Adv. Energy Mater.* **2018**, *8*(19), 1800297.
- [16] H. Jia, Y. Xu, L. Zou, P. Gao, X. Zhang, B. Taing, W. Xu, *J. Power Sources* **2022**, *527*, 231171.
- [17] G. Xu, S. Huang, Z. Cui, X. Du, X. Wang, D. Lu, G. Cui, *J. Power Sources* **2019**, *416*, 29–36.
- [18] Y. Li, K. Wang, J. Chen, W. Zhang, X. Luo, Z. Hu, Q. Zhang, L. Xing, W. Li, *ACS Appl. Mater. Interfaces* **2020**, *12*, 28169–28178.
- [19] X. He, J. Peng, Q. Lin, M. Li, W. Chen, P. Liu, T. Huang, Z. Huang, Y. Liu, J. Deng, S. Ye, X. Yang, X. Ren, X. Ouyang, J. Liu, B. Xiao, J. Hu, Q. Zhang, *Nano-Micro Lett.* **2025**, *17*, 1–19.

- [20] T. Dickinson, A. F. Povey, P. M. Sherwood, *J. Chem. Soc. Faraday Trans. 1* **1977**, *73*, 327–343.
- [21] H. Zhao, S. Hu, Y. Fan, Q. Wang, J. Li, M. Yuan, Y. Deng, *Energy Storage Mater.* **2024**, *65*, 103151.
- [22] D. Zhao, P. Wang, Q. Zhao, S. Li, Z. Zhou, *Energy Technol.* **2018**, *12*, 2450–2460.
- [23] P. Wang, Y. You, Y. Yin, Y. Guo, *J. Mater. Chem. Abstr.* **2016**, *4*, 17660–17664.
- [24] S.-M. Oh, S.-T. Myung, J.-Y. Hwang, B. Scrosati, K. Amine, Y.-K. Sun, *Chem. Mater.* **2014**, *05*, 6165–6171.
- [25] X. Sun, Y. Jin, C.Y. Zhang, J.W. Wen, Y. Shao, Y. Zang, C.H. Chen, *J. Mater. Chem. A* **2014**, *2*, 17268–17271.
- [26] S. Zhang, Y. Liu, N. Zhang, K. Zhao, J. Yang, S. He, *J. Power Sources* **2016**, *329*, 1–7.
- [27] D. Asakura, H. Niwa, H. Kiuchi, J. Miyawaki, Y. Harada, *Chem. Mater.* **2016**, *28*, 1058–1065.
- [28] S.-M. Oh, P. Oh, S.-O. Kim, A. Manthiram, *J. Electrochem. Soc.* **2017**, *164*, A321–A326.
- [29] L. Yang, J. Miguel, Z. Shadik, S. Bak, F. Bonilla, P. K. Nayak, J. R. Buchheim, X. Yang, T. Rojo, P. Adelhelm, *Adv. Funct. Mater.* **2020**, *30*, 2003364.
- [30] Q. Mao, C. Zhang, W. Yang, J. Yang, L. Sun, Y. Hao, X. Liu, *J. Alloys Compd* **2019**, *794*, 509–517.
- [31] C. Zhang, R. Gao, L. Zheng, Y. Hao and X. Liu, *ACS Appl. Energ. Mater.* **2018**, *10*, 10819–10827.

Manuscript received: September 14, 2024  
Revised manuscript received: December 18, 2024  
Accepted manuscript online: January 2, 2025  
Version of record online: January 16, 2025